Journal of Water & Health

IWA PUBLISHING

Journal of Water and Health Vol 21 No 6, 676 doi: 10.2166/wh.2023.252

Preparation of hydrogels based on poplar cellulose and their removal efficiency of Cd(II) from aqueous solutions

Fengrong Zhang [a,*], Cuilan Zhang[b], Jia Teng[a], Dandan Han[a], Lishun Wu[a] and Wanguo Hou[c]

[a] School of Chemistry and Chemical Engineering, Heze University, Heze 274015, China
[b] Guiyang Road Primary School, Heze 274015, China
[c] Key Laboratory of Colloid and Interface Chemistry (Ministry of Education), Shandong University, Jinan 250100, China
*Corresponding author. E-mail: zfrong1204@163.com

FZ, 0000-0002-4321-4776

ABSTRACT

Industrial heavy metal-contaminated wastewater is one of the main water pollution problems. Adsorbents are a promising method for the removal of heavy metal contaminants. Herein, polyaspartic acid/carboxymethyl poplar sawdust hydrogels (PASP/CMPP) and ascorbic acid/carboxymethyl poplar sawdust hydrogels (VC/CMPP) were prepared by aqueous polymerization using alkalized poplar sawdust (CMPP) as the substrate and PASP and vitamin C (VC) as modifiers. The effective results, provided by the characterization analysis of SEM and BET, indicate that the surface of the PASP/CMPP hydrogel has a larger number of loose pores and a larger pore volume than the VC/CMPP hydrogel. The treatment effects of the two hydrogels on simulated wastewater containing Cd(II) were investigated by a batch of experiments. The results showed that PASP/CMPP had a better adsorption effect than VC/CMPP under the same adsorption conditions. Interestingly, the solid concentration effect was found in the process of sorption kinetics and sorption isotherms. The sorption kinetic curves of Cd(II) on PASP/CMPP were well-fitted by the quasi-second-order kinetics under different adsorbent concentrations. The adsorption conforms to Langmuir and Freundlich adsorption isotherm models. More importantly, PASP/CMPP composites are expected to be used as a new kind of environmental adsorbent for wastewater treatment.

Key words: adsorption, heavy metal, hydrogel, solid concentration effect

HIGHLIGHTS

- Hydrogels of PASP/CMPP were prepared.
- The hydrogels of PASP/CMPP exhibit enhanced sorption capacities for Cd(II).
- The hydrogels of PASP/CMPP are potential sorbents for wastewater treatment.
- The solid concentration effect was found in the process of sorption kinetics and sorption isotherms.
- The synthesis of PASP/CMPP hydrogels provides a win-win strategy.

GRAPHICAL ABSTRACT

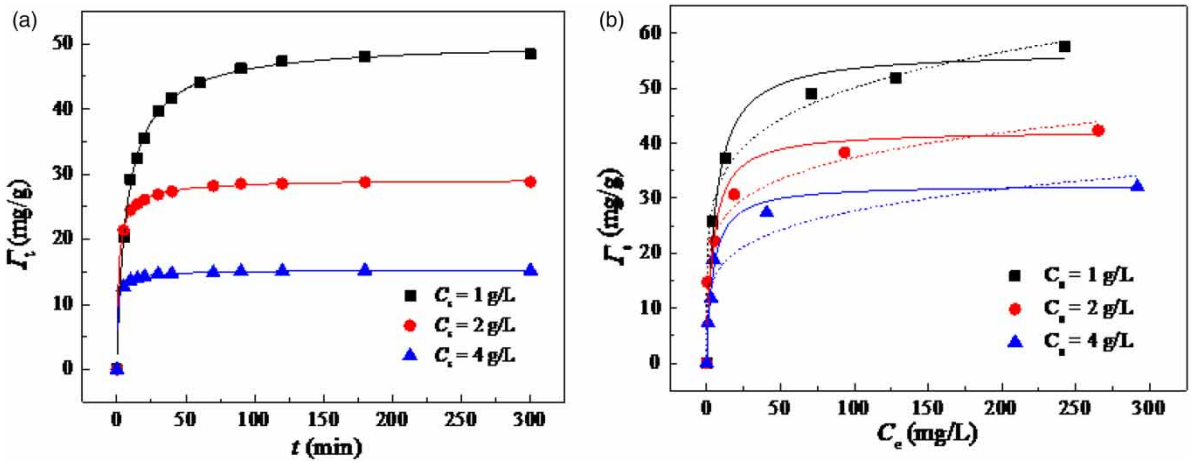

1. INTRODUCTION

Rapid industrialization and improvement of people's living standards have caused many environmental pollution problems. In reality, heavy metal ions usually coexist in environmental and industrial wastewater. Heavy metals in industrial wastewater are one of the major pollutants (Tchounwou *et al.* 2012; Shafiq *et al.* 2018; Hefny *et al.* 2020; Khan *et al.* 2021; Liu *et al.* 2022). Untreated sewage is discharged into rivers, lakes, and seas, causing serious deterioration of water quality. Heavy metals are difficult to biodegrade. Among them, cadmium (Cd), a toxic heavy metal, can be enriched in the human body through the biological diffusion effect of the food chain (Amin *et al.* 2022). Cadmium not only interacts vigorously with proteins, enzymes, and other substances in the human body, making them lose their vitality, but also accumulates in some organs of the human body, leading to slow poisoning and death (Anwar *et al.* 2010; Verma *et al.* 2018). Briefly, heavy metal water pollution not only harms human health but also reduces crop yield and quality and accelerates the degradation and destruction of the ecological environment. Heavy metal water pollution prevention and control is an urgent matter (Arumugam & Jongsung 2018; Musa *et al.* 2020).

To cope with this situation, various water treatment technologies have been explored and applied to the treatment of water pollution. The commonly used treatment methods include absorption, ion exchange, extraction, and membrane chromatography. The adsorption method is superior to other technologies in terms of initial cost, flexibility, design difficulty, operation method, and toxicity (Li *et al.* 2018; Liu *et al.* 2019; Musa & Zurina 2020; Shirell *et al.* 2020; Alharby *et al.* 2021; Tipplook *et al.* 2021; Lin *et al.* 2022). Common adsorbents are active white clay, bleaching powder, diatomaceous earth, and other natural mineral products, as well as active carbon, organic silicon, activated alumina, zeolite molecular sieve, adsorption resin, and humic acid. The use of these adsorbents has been greatly limited due to their limited adsorption capacity or difficult biodegradation.

Recently, hydrogels, as a new adsorbent, have attracted much attention (Alharby *et al.* 2021; Ma *et al.* 2021; Rahman & Rimu 2020; Wang *et al.* 2021; Weerasundara *et al.* 2021). Hydrogel is a kind of highly hydrophilic three-dimensional (3D) network structure gel (Tie *et al.* 2022). It expands rapidly in water and can hold a large volume of water without dissolving in this swelling state. Several new types of gels with excellent mechanical properties have been developed, such as topological hydrogels, double-network hydrogels, composite hydrogels, macromolecular microsphere composite hydrogels, hydrophobic association gels, and homogeneous chain hydrogels. Among them, composite hydrogels have attracted extensive attention due to their high strength and diversified composite methods. It is worth noting that the various active functional groups on the gel polymer skeleton and the 3D network structure ensure that more sites are involved in the adsorption process. These advantages of gels make them widely used as adsorbents in the field of environmental protection. The removal of heavy metal ions by hydrogels mainly depends on the presence of a large number of functional groups (such as –OH, –COOH, $–NH_2$, and $–SO_3H$) in hydrogels for adsorption, ion exchange, and chelation of heavy metal ions. The adsorption of heavy metal ions on hydrogels shows the advantages of high adsorption capacity, fast adsorption, and recycling, so the adsorption of heavy metal ions on hydrogels has become a hot spot in recent years (Wang *et al.* 2020; Kim *et al.* 2022; Muhammad *et al.* 2022; Peng *et al.* 2022; Qiu *et al.* 2022).

In order to prepare biodegradable and environmentally friendly adsorbents, it is very important to select biodegradable and environmentally friendly raw materials or environmentally friendly preparation methods (Musa *et al.* 2019; Sabet & Kamran 2019). Poplar is a kind of renewable resource in nature, which contains abundant cellulose and lignin. Cellulose and lignin contain a large number of hydroxyl, carboxyl, and other active functional groups, which play an important role in the process of adsorption (Yu *et al.* 2000; Abia *et al.* 2003; Abdić *et al.* 2018). Polyaspartic acid (PASP) belongs to a group of polyamino acids (Yang *et al.* 2019). PASP is easily broken by microorganisms and fungi because of the peptide bonds in its structural backbone, and the final degradation products are ammonia, carbon dioxide, and water, which are harmless to the environment (Jv *et al.* 2019). Therefore, it is widely used (Ye & Wang 2016; Hao & Li 2019). It can be used in water treatment, medicine, agriculture, daily chemical, and other fields. As a new green water treatment agent, it can chelate calcium, magnesium, copper, and other multivalent metal ions. Vitamin C (VC) is a polyhydroxyl compound. The molecular structure of VC has an enediol structure, a lactone ring, and two chiral carbon atoms. Therefore, it is not only active in nature but also has an optical rotation.

In this study, PASP/CMPP hydrogels and VC/CMPP hydrogels were prepared by using glutaraldehyde as a cross-linking agent, and used for the treatment of wastewater containing Cd(II), in order to understand the removal behavior of Cd(II) by hydrogels. Therefore, the main objective is to compare the removal efficiencies and adsorption capacities between PASP/CMPP and VC/CMPP on the adsorption properties of Cd(II).

2. EXPERIMENTAL SECTION

2.1. Reagents

NaOH and $KMnO_4$ were purchased from Tianjin Damao Chemical Pharmacy Factory. PASP, glutaraldehyde, $Cd(NO_3)_2$, and VC were purchased from Aladdin Reagent (Shanghai) Co., Ltd, China. Anhydrous ethanol was purchased from Tianjin Kermel Chemical Reagent Co., Ltd, China. Potassium bromide, HNO_3, and CH_3COOH were purchased from Sinopharm Chemical Reagent Co., Ltd, China. All chemicals were used without further purification. The poplar was collected from the north side of the comprehensive experimental building on the campus of Heze University. Water was purified with a Hitech-Kflow water purification system (Hitech, China).

2.2. Preparation of CMPP, PASP/CMPP, and VC/CMPP composites

First, the collected poplar was washed with water to remove the dust and dried in an electric thermostatic air-blowing drying oven. Second, it was pulverized with a pulverizer, sifted through a 100-mesh sieve, and then set aside. Third, 2 g of poplar sawdust was weighed and immersed in 100 mL of 15% NaOH solution for 12 h. Fourth, the mixture was centrifuged, washed, and then transferred to a round-bottom flask. Finally, 20 mL of ethanol and 2 mL of acetic acid were added and the mixture was stirred using a magnetic stirrer for 30 min at room temperature. The final sample obtained is denoted as CMPP.

0.1 g CMPP was weighed and added to 50 mL of 0.06 mol/L $KMnO_4$ solution, and the mixture was stirred using a magnetic stirrer at 50 °C for 15 min. Under the conditions of continuous magnetic stirring at 70 °C for 3.5 h, 1.5 g of PASP and 1 g of glutaraldehyde were measured and added to the above solution. The sample was frozen and lyophilized in a freeze dryer for 72 h. The material obtained after freeze-drying is denoted as the PASP/CMPP hydrogel. For comparison, VC/CMPP was prepared in the same way by substituting PASP for VC.

2.3. Characterization

The sample morphology was analyzed using a JSM-6700F scanning electron microscope (SEM, JEOL, Japan) under the conditions of 1 kV acceleration voltage and gold spraying. Fourier transform infrared spectra (FTIR) (Nicolet 5700 Spectrometer, USA) of samples were recorded in the range of 500–3,900 cm^{-1}. The N_2 adsorption–desorption isotherms were determined using a Autosorb IQ-MP system (Quantachrome Instruments, USA), and the test samples were degassed at 120 °C for 5 h under vacuum before measurement. The specific surface area (A_s) and pore volume (V_p) of the samples were calculated using the Brunauer–Emmett–Teller (BET) and Barrett–Joyner–Halenda (BJH) methods, respectively.

2.4. Sorption experiments

The heavy metal ion, Cd(II), was used as the target to test the adsorption capacity. The cadmium removal test was carried out at room temperature. The initial concentrations of Cd(II) from 30 to 300 mg/L were prepared by dissolving $Cd(NO_3)_2$ in deionized water. A certain amount of adsorbent was weighed and put into a polyethylene tube containing a certain volume of the

above solution and oscillated at 150 r/min in a thermostatic oscillator until the specified time. The initial pH values of the solutions were adjusted to 5.5 with 1 mol/L of HCl and 1 mol/L of NaOH solution. Then, an appropriate amount of the solution was filtered through a 0.45-μm filter membrane, and the concentration of cadmium ions present in the filtrate was tested by an atomic absorption spectrophotometer (AAS) (AAS-3600, Shanghai Metash Instruments Co., Ltd, China) equipped with an air-acetylene flame.

In order to investigate the time required to reach adsorption equilibrium, samples were taken at the following times: 5 min,10 min, 15 min, 20 min, 30 min, 40 min, 60 min, 90 min, 2 h, 3 h, and 5 h, respectively. The adsorption amounts (Γ_t) at different times were calculated as follows:

$$\Gamma_t = \frac{(C_0 - C_t)}{C_s} \tag{1}$$

where the C_0 (mg L^{-1}) is the initial concentration and C_t is the concentration of the solution at time t. C_s (g L^{-1}) is the sorbent dosage.

To ensure sorption equilibrium, the adsorption time (t) was selected as 24 h in the equilibrium sorption tests. The equilibrium adsorption amount (Γ_e) and the removal efficiency in this study were calculated as follows:

$$\Gamma_e = \frac{(C_0 - C_e)}{C_s} \tag{2}$$

$$\text{Efficiency } (\%) = \frac{(C_0 - C_e)}{C_0} \times 100\% \tag{3}$$

where the C_e refers to the concentration of solution at adsorption equilibrium.

The tests shall be conducted three times and the average of overall measurements was taken as the final value, with a relative error less than 5.2%.

3. RESULTS AND DISCUSSION

3.1. Characterizations

3.1.1. SEM analysis

Figure 1 presents the SEM images of samples. As Figure 1(a) shows, there is a lot of interlacing cellulose in poplar. After the reaction of alkalized poplar wood with absolute ethanol and acetic acid, the structure of cellulose in poplar wood changed obviously, and the CMPP appeared granular (Figure 1(b)). The surface of PASP/CMPP hydrogel has a large number of loose pores (Figure 1(c)), while the VC/CMPP hydrogel shows a bulk structure (Figure 1(d)). This indicates that PASP and VC play an important role in the process of gel formation. Although both of them are polyhydroxyl compounds, the presence of PASP makes the samples more porous and loose.

3.1.2. FTIR analysis

Figure 2 presents FTIR spectra of the following samples: poplar, CMPP, VC/CMPP, PASP/CMPP. Poplar only had a characteristic peak at 1,038 cm^{-1}, which was assigned to O–H bending vibration and C–O–C stretching vibration (Ye & Wang 2016). However, the modified poplar wood showed more characteristic peaks, and the characteristic peaks at 799; 1,410; 1,025; and 1,547 cm^{-1} were designated as the –OH, –CH, –COOH, and $-CH_2OH$ tensile vibrations of CMPP. After CMPP copolymerizes with VC and PASP, the position of each characteristic peak changes significantly. The absorption peaks at 799 and 1,547 cm^{-1} move to high wave numbers 808 and 1,628 cm^{-1}, respectively. Also, the absorption peaks at 1,025 and 1,410 cm^{-1} disappear and are replaced by 1,310 and 1,361 cm^{-1}, respectively. In the sample of PASP/CMPP, there are only absorption peaks at 1,398 and 1,548 cm^{-1}. The above results implied that VC and PASP have successfully combined with CMPP.

3.1.3. BET analysis

Figure 3 shows the N_2 adsorption–desorption isotherms of CMPP, VC/CMPP, and PASP/CMPP samples. The surface area (A_s), average pore size (D_p), and pore volume (V_p) of the samples are listed in Table 1. The specific surface areas of VC/CMPP

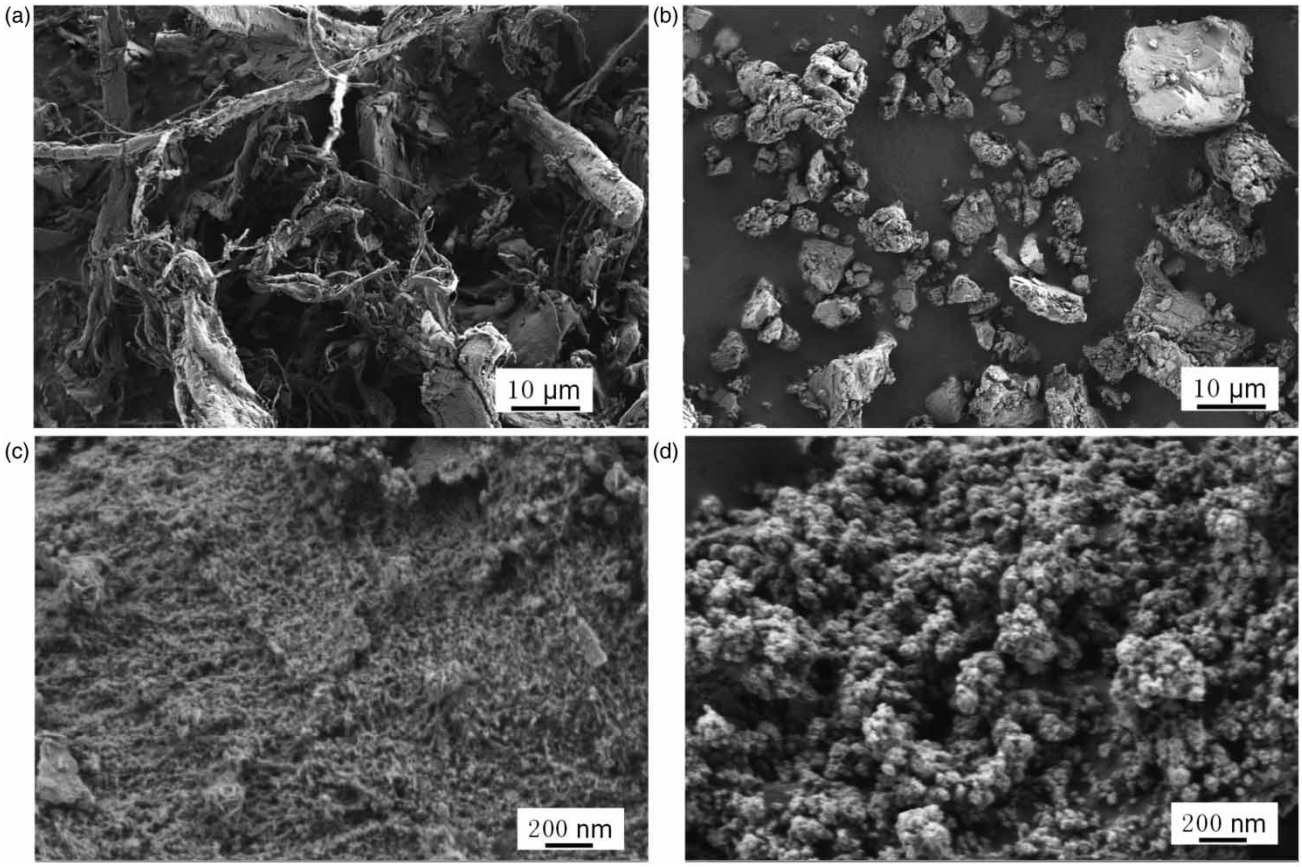

Figure 1 | SEM images of the following samples: (a) poplar; (b) CMPP; (c) PASP/CMPP; (d) VC/CMPP.

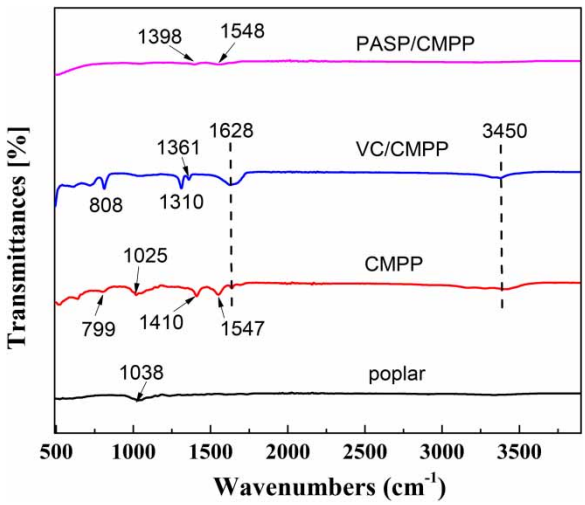

Figure 2 | FTIR spectra of the following samples: poplar; CMPP; VC/CMPP; PASP/CMPP.

and PASP/CMPP are 0.54 and 9.96 m^2g^{-1}, respectively. The curves of all samples showed that the adsorption line rose gently and the desorption line fell gently. This indicates that the pore structure in the sample is made up of pores, which are formed by plates that are tilted to each other. In addition, the average pore size (D_p) and pore volume (V_p) of samples are 4.37 nm and

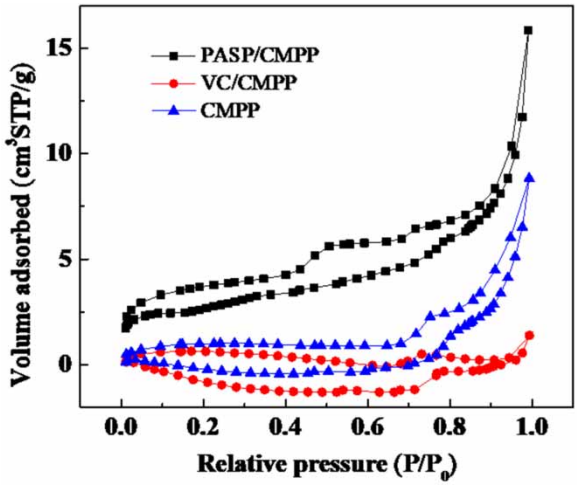

Figure 3 | N_2 adsorption–desorption isotherms of CMPP, VC/CMPP, and PASP/CMPP samples.

Table 1 | Specific surface area, average pore size, and pore volume of samples

Samples	A_s (m^2/g)	D_p (nm)	V_p (cm^3/g)
PASP/CMPP	9.96	4.37	0.009
VC/CMPP	0.54	5.80	0.0008
CMPP	0.30	8.06	0.004

0.009 cm^3g^{-1} for PASP/CMPP, and 5.80 nm and 0.0.0008 cm^3g^{-1} for VC/CMPP, respectively. By comparison, it is found that the PASP/CMPP sample has a larger pore volume, which is also conducive to adsorption. What's more, the CMPP sample has a smaller specific surface area and pore volume, which are not conducive to adsorption.

3.2. The results on Cd(II) adsorption

The removal efficiency of CdII) by different adsorbents of CMPP, VC/CMPP, and PASP/CMPP were investigated at $C_0 = 50$ mg/L, $C_s = 1.0$ g/L, pH = 5.5, and 25 °C (Figure 4). The removal efficiency of PASP/CMPP was 93.69%, which was the best among the three sorbents for Cd(II) removal. The removal efficiency of CMPP and VC/CMPP were 8.84 and 3.96%, respectively. The specific surface area of PASP/CMPP is the largest among the three, which may be one of the reasons for the highest removal efficiency. Although some pores exist in VC/CMPP hydrogels, they hardly play a role in the adsorption process. Moreover, the addition of VC destroys part of the pore structure in CMPP, and results in the lowest removal effect. The above results are consistent with the results of BET analysis (see Section 3.1.3).

The solid concentrations are an important factor affecting the adsorption effect (O'Connor & Connolly 1980; Voice & Weber 1985). It is of great theoretical and practical significance to study the effect of sorbent dosage on adsorption performance. Figure 5 shows the sorption kinetic curves and sorption isotherms of PASP/CMPP adsorbing Cd(II) at different solid concentrations under conditions of 25 °C and pH = 5.5. The adsorption results show that the adsorption amount decreases with the increase of the amount of adsorbent. The C_s dependence of the sorption isotherms is a well-known solid (or sorbent concentration) effect (C_s effect) (Zhao & Hou 2012; Zhao *et al.* 2013).

Langmuir and Freundlich isotherms were used to fit the adsorption data of different C_s values with nonlinear regression. The Langmuir model can be expressed in a nonlinear form as,

$$\Gamma_e = \frac{K_L \Gamma_m C_e}{1 + K_L C_e} \tag{4}$$

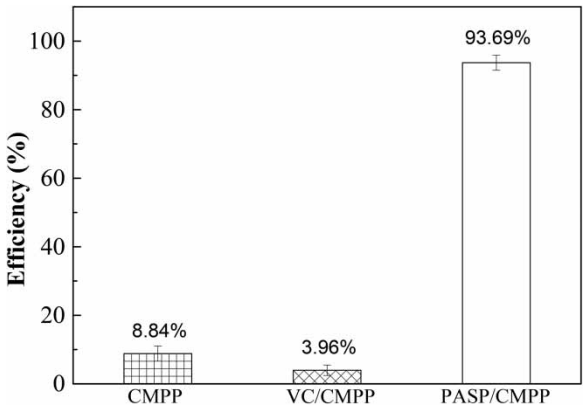

Figure 4 | The removal efficiency of Cd(II) by different adsorbents of CMPP, VC/CMPP, and PASP/CMPP samples ($C_0 = 50$ mg/L, $C_s = 1.0$ g/L, pH = 5.5, and 25 °C).

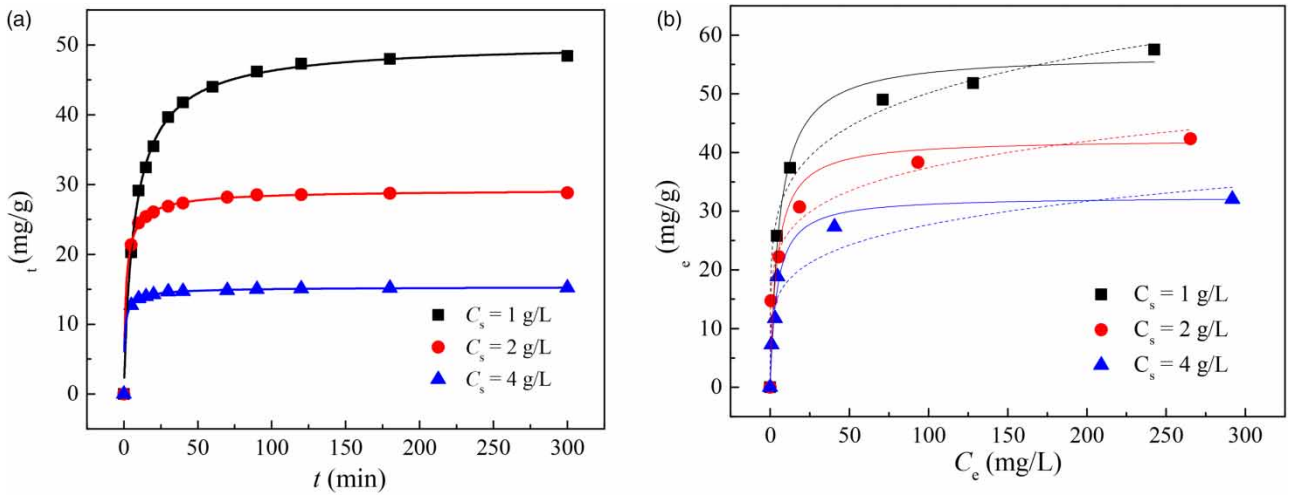

Figure 5 | Cd(II) adsorbed on PASP/CMPP at different sorbent concentrations: (a) sorption kinetics curves and (b) sorption isotherms. (The dots represent experimental data, the solid lines represent Langmuir model fits, and the dashed lines represent Freundlich model fits. 25 °C, pH = 5.5.)

or in a linear form as,

$$\frac{C_e}{\Gamma_e} = \frac{C_e}{\Gamma_m} + \frac{1}{K_L \Gamma_m} \tag{5}$$

The Freundlich model can be expressed in a nonlinear form as,

$$\Gamma_e = K_F C_e^{n_F} \tag{6}$$

or in a linear form as,

$$lg\,\Gamma_e = lg\,K_F + n_F\,lg\,C_e \tag{7}$$

The sorption data for the various composites were fitted using the Langmuir and Freundlich isotherms using nonlinear and linear regressions. All of the nonlinear model plots coincided with the experimental data (Figure 5(b)), and the linear model

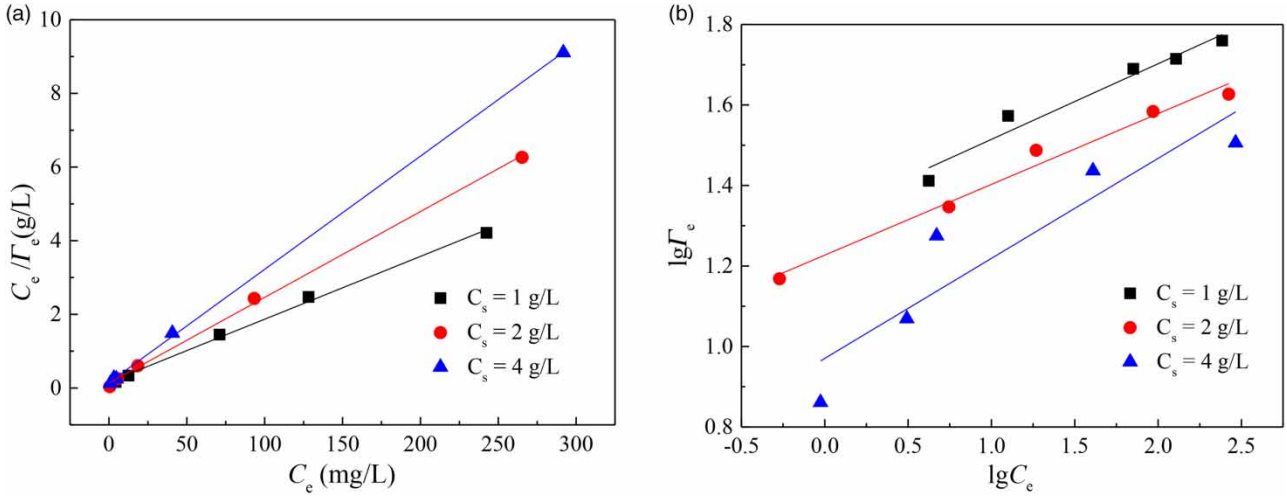

Figure 6 | Linear correlation plots of (a) Langmuir and (b) Freundlich isotherms for Cd(II) sorption on PASP/CMPP at different C_s values.

Table 2 | Nonlinear-fit data of model parameters for Cd(II) sorption on PASP/CMPP at different C_s values

	Langmuir isotherm			Freundlich isotherm		
C_s (g/L)	Γ_m (mg/g)	K_L (L/mg)	R^2	K_F L^{nF} (mg^{1-nF}/g)	n_F	R^2
1.00	56.8	0.168	0.987	22.4	0.175	0.989
2.00	42.3	0.230	0.903	17.7	0.163	0.988
4.00	32.5	0.234	0.982	11.3	0.194	0.909

plots were straight lines (Figure 6). Table 2 and Table 3 list the best-fit values of the model parameters, Γ_m, K_L, K_F, n_F, and R^2. Higher R^2 values for the various model-fitting plots indicated that the Langmuir and Freundlich models adequately described the sorption isotherms for any given C_s value. Furthermore, Table 2 and Table 3 show that the Γ_m values decreased with increasing C_s. Similar results were reported in our previous studies (Zhang *et al.* 2015, 2019, 2021).

When describing the adsorption phenomenon at the solid–liquid interface, the quasi-first-order rate equation (Ho 2004) and quasi-second-order rate equation (Ho & McKay 1999) can be expressed as the following equations:

$$\Gamma_t = \Gamma_e(1 - e^{-k_1 t}) \tag{8}$$

$$\Gamma_t = \frac{\Gamma_e^2 k_2 t}{1 + \Gamma_e k_2 t} \tag{9}$$

where k_1 (1/h) and k_2 (g/(mg·h)) are the quasi-first-order and quasi-second-order rate equation adsorption rate constants, respectively. All of the linear model plots coincided with the experimental data (Figure 7). Table 4 lists the best-fit values

Table 3 | Linear-fit data of model parameters for Cd(II) sorption on PASP/CMPP at different C_s values

	Langmuir isotherm			Freundlich isotherm		
C_s (g/L)	Γ_m (mg/g)	K_L (L/mg)	R^2	K_F (L^{nF}·mg^{1-nF}/g)	n_F	R^2
1.00	58.6	0.104	0.996	21.2	0.188	0.947
2.00	42.9	0.176	0.998	16.9	0.176	0.977
4.00	32.5	0.204	0.999	9.34	0.248	0.809

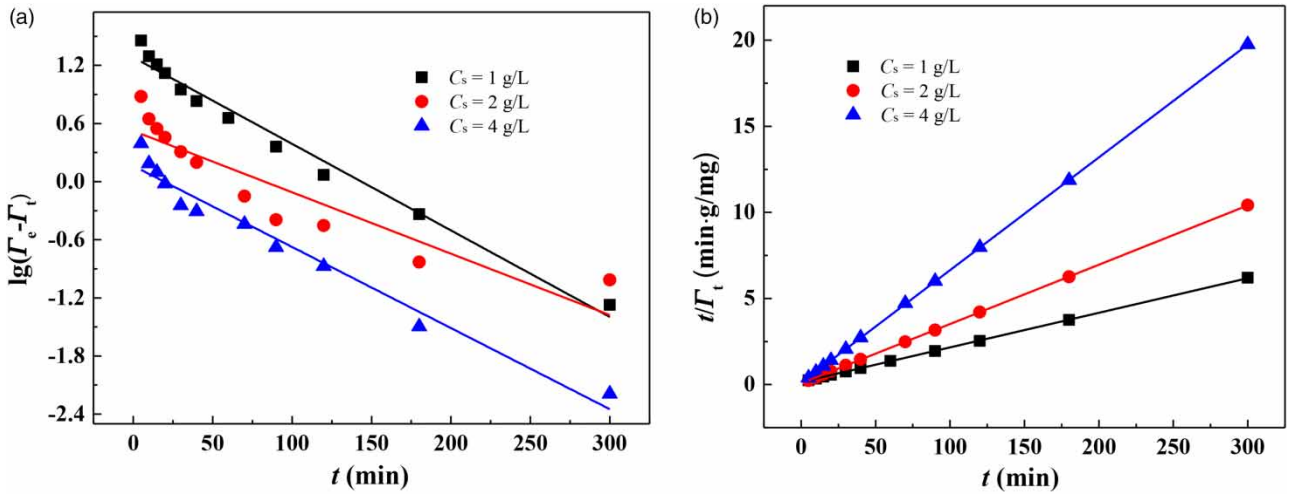

Figure 7 | Cd(II) adsorbed on PASP/CMPP at different sorbent concentrations: (a) quasi-first-order kinetic fitting and (b) quasi-second-order kinetic fitting (25 °C, pH = 5.5).

Table 4 | Quasi-first-order kinetic fit and quasi-second-order kinetic fit data of model parameters for Cd(II) sorption on PASP/CMPP at different C_s values

	Quasi-first-order kinetic fit			Quasi-second-order kinetic fit		
C_s (g/L)	$\Gamma_{e,1}$(mg/g)	k_1(min^{-1})	R^2	$\Gamma_{e,2}$(mg/g)	k_2(gmg^{-1}min^{-1})	R^2
1.00	19.2	0.0205	0.9783	49.8	0.0027	0.9999
2.00	3.35	0.0146	0.8289	29.0	0.0166	0.9999
4.00	1.46	0.0193	0.9647	15.3	0.0469	0.9999

of the quasi-first-order rate equation and quasi-second-order rate equation. Higher R^2 values for the various model-fitting plots indicated that the quasi-second-order rate equation adequately described the sorption kinetics curves for any given C_s value, which is better than the quasi-first-order rate equation.

4. CONCLUSIONS

The PASP/CMPP hydrogel was successfully synthesized by using alkalized poplar sawdust (CMPP) as the substrate and PASP as the modifier. The effective results, provided by the characterization analysis of SEM and BET, indicate that the surface of the PASP/CMPP hydrogel has a large number of loose pores and a larger pore volume, which are conducive for adsorption. Under the same adsorption conditions, the adsorption capacity of the PASP/CMPP hydrogel was higher than that of the VC/CMPP hydrogel. The sorption kinetics for Cd(II) follow a pseudo-second-order, and sorption isotherms follow the Langmuir and Freundlich models. There is an obvious effect of solid concentrations on the sorption kinetic curves and sorption isotherms. The PASP/CMPP hydrogel has a promising application in the removal of Cd(II) in water. This research provides insights into the synthesis of an efficient and biodegradable functional adsorbent for the simultaneous removal of heavy metal pollutants in wastewater.

ACKNOWLEDGEMENTS

This work is supported financially by the Science and Technology Program for Colleges and Universities of Shandong Province (No. J18KA104).

AUTHOR CONTRIBUTION

F.Z. conceived and designed the experiment. She performed the experiments and carried out the data analysis. J.T. and D.H. carried out characterization experiments on the samples. L.W., C.Z., and W.H. have polished the grammar of the manuscript. All authors have read and agreed to the published version of the manuscript.

DATA AVAILABILITY STATEMENT

All relevant data are included in the paper or its Supplementary Information.

CONFLICT OF INTEREST

The authors declare there is no conflict.

REFERENCES

Abdić, Š., Memić, M., Šabanović, E., Sulejmanović, J. & Begić, S. 2018 Adsorptive removal of eight heavy metals from aqueous solution by unmodified and modified agricultural waste: tangerine peel. *International Journal of Environmental Science and Technology* **15**, 2511–2518.

Abia, A. A., Horsfall, M. & Didi, O. 2003 The use of chemically modified and unmodified cassava waste for the removal of Cd, Cu and Zn ions from aqueous solution. *Bioresource Technology* **90**, 345–348.

Alharby, N. F., Almutairi, R. S. & Mohamed, N. A. 2021 Adsorption behavior of methylene blue dye by novel crosslinked o-cm-chitosan hydrogel in aqueous solution: kinetics, isotherm and thermodynamics. *Polymers* **13** (21), 3659.

Amin, M. T., Alazba, A. A. & Shafiq, M. 2022 Ethylenediaminetetraacetate functionalized MgFe layered double hydroxide/biochar composites for highly efficient adsorptive removal of lead ions from aqueous solutions. *Plos One* **17** (3). https://doi.org/10.1371/journal.pone.0265024.

Anwar, J., Shafique, U., Waheed, Z., Salman, M., Dar, A. & Anwar, S. 2010 Removal of Pb(II) and Cd(II) from water by adsorption on peels of banana. *Bioresource Technology* **101**, 1752–1755.

Arumugam, N. & Jongsung, K. 2018 Synthesis of carbon quantum dots from Broccoli and their ability to detect silver ions. *Materials Letters* **219**, 37–40.

Hao, W. & Li, W. 2019 Preparation of PASP/SPP hydrogels with high adsorption capacity for Pb(II). *Desalination and Water Treatment* **170**, 277–286.

Hefny, R., Ibrahim, M. M. & Morad, D. 2020 Study of adsorption performance of biochar for heavy metals removal. *Journal of Engineering Research and Reports* **19**, 27–40.

Ho, Y. 2004 Citation review of Lagergren kinetic rate equation on adsorption reactions. *Scientometrics* **59** (1), 171–177.

Ho, Y. S. & McKay, G. 1999 Pseudo-second order model for sorption processes. *Process Biochemistry* **34** (5), 451–465.

Jv, X., Zhao, X., Ge, H., Sun, J., Li, H., Wang, Q. & Lu, H. 2019 Fabrication of a magnetic poly(aspartic acid)-poly(acrylic acid) hydrogel: application for the adsorptive removal of organic dyes from aqueous solution. *Journal of Chemical and Engineering Data* **64** (3), 1228–1236.

Khan, Z. U., Khan, W. U., Ullah, B., Ali, W., Ahmad, B., Ali, W. & Yap, P. S. 2021 Graphene oxide/PVC composite papers functionalized with p-Phenylenediamine as high-performance sorbent for the removal of heavy metal ions. *Journal of Environmental Chemical Engineering* **9**, 105916.

Kim, Y., Bang, J., Kim, J., Choi, J., Hwang, S., Yeo, H., Choi, I., Jin, H. & Kwak, H. W. 2022 Cationic surface-modified regenerated nanocellulose hydrogel for efficient Cr(VI) remediation. *Carbohydrate Polymers* **278**, 118930.

Li, R., Wang, J. J., Gaston, L. A., Zhou, B., Li, M., Xiao, R., Wang, Q., Zhang, Z., Huang, H., Liang, W., Huang, H. & Zhang, X. 2018 An overview of carbothermal synthesis of metal-biochar composites for the removal of oxyanion contaminants from aqueous solution. *Carbon* **129**, 674–687.

Lin, Z., Shen, W., Corriou, J. P., Chen, X. & Xi, H. 2022 Assessment of multiple environmental factors on the adsorptive and photocatalytic removal of gaseous formaldehyde by a nano-TiO_2 colloid: experimental and simulation studies. *Journal of Colloid and Interface Science* **608**, 1769–1781.

Liu, Y., Hu, L., Tan, B., Li, J., Gao, X., He, Y., Du, X., Zhang, W. & Wang, W. 2019 Adsorption behavior of heavy metal ions from aqueous solution onto composite dextran-chitosan macromolecule resin adsorbent. *International Journal of Biological Macromolecules* **141**, 738–746.

Liu, T., Lawluvy, Y., Shi, Y., Ighalo, J. O., He, Y., Zhang, Y. & Yap, P. S. 2022 Adsorption of cadmium and lead from aqueous solution using modified biochar: a review. *Journal of Environmental Chemical Engineering* **10**, 106502.

Ma, J., Zhang, M., Ji, M., Zhang, L., Qin, Z., Zhang, Y., Gao, L. & Jiao, T. 2021 Magnetic grapheme oxide-containing chitosan sodium alginate hydrogel beads for highly efficient and sustainable removal of cationic dyes. *International Journal of Biological Macromolecules* **193** (15), 2221–2231.

Muhammad, K. A., Muhammad, R., Atif, I., Atta, R., Shahzad, M. K., Rafi, U. K., Tahir, R. & Muhammad, B. 2022 In-house fabrication of macro-porous biopolymeric hydrogel and its deployment for adsorptive remediation of lead and cadmium from water matrices. *Environmental Research* **214**, 113790.

Musa, Y. P. & Zurina, Z. A. 2020 A sustainable and eco-friendly technique for dye adsorption from aqueous. *Desalination and Water Treatment* **182**, 1–10.

Musa, Y. P., Zurina, Z. A., Suraya, A. R., Faizah, M. Y., Noor, A. S. M. & Mohammed, A. 2019 Synthesis and characterization of fluorescent carbon dots from Tapioca. *Chemistry Select* **4**, 1–8.

Musa, Y. P., Zurina, Z. A., Suraya, A. R., Faizah, M. Y., Noor, A. S. M. & Mohammed, A. 2020 Eco-Friendly sustainable fluorescent carbon dots for the adsorption of heavy metal ions in aqueous environment. *Nanomaterials* **10**, 315–334.

O'Connor, D. J. & Connolly, J. P. 1980 The effect of concentration of adsorbing solids on the partition coefficient. *Water Research* **14**, 1517–1523.

Peng, J., Yuan, H., Ren, T., Liu, Z., Qiao, J., Ma, Q., Guo, X., Ma, G. & Wu, Y. 2022 Fluorescent nanocellulose-based hydrogel incorporating titanate nanofibers for sorption and detection of Cr(VI). *International Journal of Biological Macromolecules* **215**, 625–634.

Qiu, Z., Fu, K., Yu, D., Luo, J., Shang, J., Luo, S. & Crittenden, J. C. 2022 Radix Astragali residue-derived porous amino-laced double network hydrogel for efficient Pb(II) removal: performance and modeling. *Journal of Hazardous Materials* **438**, 129418.

Rahman, M. M. & Rimu, S. H. 2020 Recent development in cellulose nanocrystal-based hydrogel for decolouration of methylene blue from aqueous solution: a review. *International Journal of Environmental Analytical Chemistry*. https://doi.org/10.1080/03067319.2020.1817424.

Sabet, M. & Kamran, M. 2019 Green synthesis of high photoluminescence nitrogen-doped carbon quantum dots from grass via a simple hydrothermal method for removing organic and inorganic water pollutions. *Applied Surface Science* **463**, 283–291.

Shafiq, M., Alazba, A. A. & Amin, M. T. 2018 Removal of heavy metals from wastewater using date palm as a biosorbent: a comparative review. *Sains Malaysiana* **47**, 35–49.

Shirell, E. K., Sosa, J. D., Alexander, C., Flores, W. I., Zarzar, L. D. & Liu, Y. 2020 Green synthesis of Zr-based metal–organic framework hydrogel composites and their enhanced adsorptive properties. *Inorganic Chemistry Frontiers* **7**, 4813–4821.

Tchounwou, P. B., Yedjou, C. G., Patlolla, A. K. & Sutton, D. J. 2012 Heavy metals toxicity and the environment. *Molecular, Clinical and Environmental Toxicology* **101**, 133–164.

Tie, L., Ke, Y., Gong, Y., Zhang, W. & Deng, Z. 2022 Nanocellulose fine-tuned poly(acrylic acid) hydrogel for enhanced diclofenac removal. *International Journal of Biological Macromolecules* **213**, 1029–1036.

Tipplook, M., Sudare, T., Shiiba, H., Seki, A. & Teshima, K. 2021 Single-step topochemical synthesis of NiFe layered double hydroxides for superior anion removal from aquatic systems. *ACS Applied Materials & Interfaces* **13**, 51186–51197.

Verma, R., Vijayalakshmy, K. & Chaudhiry, V. 2018 Detrimental impacts of heavy metals on animal reproduction: a review. *Journal of Entomology and Zoology Studies* **6**, 27–30.

Voice, T. C. & Weber, W. J. 1985 Sorbent concentration effects in liquid/solid partitioning. *Environmental Science and Technology* **19**, 789–796.

Wang, Y., Yu, L., Wang, R., Wang, Y. & Zhang, X. 2020 A novel cellulose hydrogel coating with nanoscale FeO for Cr(VI) adsorption and reduction. *Science of the Total Environment* **726**, 138625.

Wang, Z., Li, T. T., Peng, H. K., Ren, H. T., Lou, C. W. & Lin, J. H. 2021 Low-cost hydrogel adsorbent enhanced by trihydroxy melamine and β-cyclodextrin for the removal of Pb (II) and Ni (II) in water. *Journal of Hazardous Materials* **411**, 125029.

Weerasundara, L., Gabriele, B., Figoli, A., Ok, Y. S. & Bundschuh, J. 2021 Hydrogels: novel materials for contaminant removal in water-a review. *Environmental Science and Technology* **51**, 1970–2014.

Yang, Z., Yu, M., Liu, Y., Chen, X. & Zhao, Y. 2019 Synthesis and performance of an environmentally friendly polycarboxylate superplasticizer based on modified poly(aspartic acid). *Construction and Building Materials* **202**, 154–161.

Ye, M. H. & Wang, L. 2016 Preparation and absorption properties of polyaspartic acid/lignocellulose hydrogels. *Acta Materiae Compositae Sinica* **33** (09), 2094–2210.

Yu, B., Zhang, Y., Shukla, A., Shukla, S. S. & Dorris, K. L. 2000 The removal of heavy metal from aqueous solutions by sawdust adsorption – removal of copper. *Journal of Hazardous Materials* **B80**, 33–42.

Zhang, F., Song, Y., Song, S., Zhang, R. & Hou, W. 2015 Removal of Pb(II) and 2,4-dichlorophenoxyacetic acid from aqueous solutions using magnetite-graphene oxide-layered double hydroxide composites. *ACS Applied Materials & Interfaces* **7** (13), 7251–7263.

Zhang, F., Han, D., Guo, Q. & Hou, W. 2019 Fabrication of layered double hydroxide/silica foam nanocomposites and their application for removing Pb(II) and Cr(VI) from aqueous solutions. *Chemistry Select* **4**, 6971–6977.

Zhang, F., Zhang, B., Han, D., Wu, L. & Hou, W. 2021 Preparation of composite soybean straw-based materials by LDHs modifying as a solid sorbent for removal of Pb(II) from water samples. *Open Chemistry* **19**, 726–734.

Zhao, L. & Hou, W. 2012 The effect of sorbent concentration on the partition coefficient of pollutants between aqueous and particulate phases. *Colloids Surface A* **396**, 29–34.

Zhao, L., Song, S., Du, N. & Hou, W. 2013 A sorbent concentration dependent Freundlich isotherm. *Colloid and Polymer Science* **291**, 541–550.

First received 2 October 2022; accepted in revised form 3 May 2023. Available online 15 May 2023